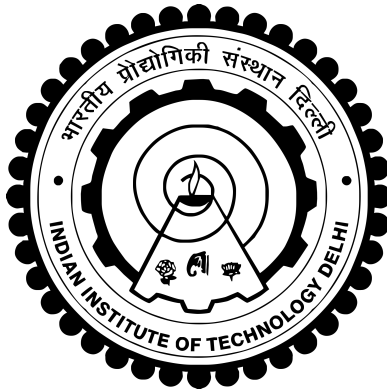


**OPERATION OF CASCADED H-BRIDGE
MULTILEVEL CONVERTER FOR GRID
CONNECTED SOLAR PV AND MOTOR DRIVE
APPLICATIONS**

RAHUL SHARMA



**DEPARTMENT OF ELECTRICAL ENGINEERING
INDIAN INSTITUTE OF TECHNOLOGY DELHI
DECEMBER 2020**

© Indian Institute of Technology Delhi (IITD), New Delhi, 2020

**OPERATION OF CASCADED H-BRIDGE
MULTILEVEL CONVERTER FOR GRID
CONNECTED SOLAR PV AND MOTOR DRIVE
APPLICATIONS**

by

RAHUL SHARMA

Department of Electrical Engineering

Submitted

in fulfillment of the requirement of the degree of **DOCTOR OF PHILOSOPHY**

to the



**INDIAN INSTITUTE OF TECHNOLOGY DELHI
DECEMBER 2020**

To my teacher, family and friends ...

Certificate

This is to certify that the thesis entitled “**Operation of Cascaded H-bridge Multilevel Converter for Grid Connected Solar PV and Motor Drive Applications**”, submitted by **Mr. Rahul Sharma (Entry No. : 2016EEZ8088)** to the Indian Institute of Technology Delhi, for the award of the degree of **Doctor of Philosophy** in Electrical Engineering, is a record of the original, bona fide research work carried out by him under our supervision and guidance. The thesis has reached the standards fulfilling the requirements of the regulations related to the award of the degree.

The results contained in this thesis have not been submitted in part or in full to any other University or Institute for the award of any degree or diploma to the best of our knowledge.

Date:

(Dr. Anandarup Das)

Department of Electrical Engineering,
Indian Institute of Technology Delhi.
Hauz Khas, New Delhi-110016, India.

Acknowledgements

I would like to express my sincere gratitude and deepest appreciation to my supervisor, **Dr. Anandarup Das**, who gave me the opportunity which allowed this thesis to become a reality. Thanks for the constant support, guidance, invaluable help and encouragement to never stop throughout the course of my study, no matter how hard things could be. Working under him has been a wonderful experience, which has provided a deep insight to the world of research. Determination, dedication, innovativeness, resourcefulness and discipline of **Dr. Anandarup Das** have been the inspiration for me to complete this work. Due to his blessing, I have earned various experiences other than research which will help me throughout my life.

I would like to thank my SRC committee members **Dr. Amit Kumar Jain**, **Dr. Ramkrishan Maheshwari**, and **Dr. Ashu Verma** for their constant support and time in evaluating my thesis during my research work.

My special thanks to the research project sponsored by the SERB, Department of Science & Technology, Govt. of India, project titled: **Design and Development of Fault Tolerant Modular Multilevel Power Electronic Converters for Grid Connected Applications** for funding my research work.

I wish to convey my sincere thanks to **Dr. Amit Kumar Jain**, and **Prof. M. Veerachary** for their valuable inputs during my course work which made the foundation for my research work. I am grateful to IIT Delhi for providing me the research facilities.

I am also thankful to Sh. Dhanraj Singh and Late Sh. Suresh Kumar of UG Machines and Drives Lab, IIT Delhi for their technical assistance during the course of my work.

I would like to thank my seniors Dr. Himanshu Misra, Dr. Kapil Shukla, Dr. Prasun Mishra, Dr. B. Nikhil Krishna , Mrs. Nibedita Parida, Mr. Tasadug Hussein, Mr. P. R.

Ghosh, Mrs. Nidhi Mishra, Mrs. Radha khushwaha, Mr. Piyush kant, Mrs Poonam Jayal, Mr. Sreejith and Ms. Neha tak to motivate me during my research work. I would also like to thank Mr. Harsha Vardhan who has helped me during the initial phase of my research. I would like to use this opportunity to thank Ms. Rashmi Rai who always believed in me and constantly helped me on all technical and non-technical issues. I would like to thank Mrs. Nidhi Bisht, Mr. E. C. Mathew, Ms. Khusbhoo Kumari, Mr. Navneet Vaishnav, Mr. Aamir Rafiq, Mr. Himanshu Swami, Mr. Vishal kumar, Mr. Rajat Kumar, Mr. Subhasis Nayak, Mr. Sukrashis Sarkar Ms. Cheshta Jain, and all other colleagues of U.G Machines and Drives Lab for their valuable help and co-operation. My friends Ms. Rashmi Rai, Mr. Pritam Mahawar, Mr. Prashant Singh, and Mrs. Subarni Pradhan that I have found on my way and I am lucky to be able to conserve them for my whole life. I would also like to thank Mr. Satish, Mr. Yatindra, and all other electrical engineering office staff for being supportive throughout my study. I am likewise thankful to those who have directly or indirectly helped me to finish my dissertation study.

I would like to thank my parents, Smt. Koshalya Devi and Sh. Kajod Mal Sharma for their support, blessings and endless love. Moreover, I would like to thank all my family members for being such a special family that I am proud to be a part of. Their trust in my capabilities had been a key factor to all my achievements.

At last, I am beholden to almighty for their blessings to help me to raise my academic level to this stage. I pray for their benediction in my future endeavours. Their blessings may be showered on me for strength, wisdom and determination to achieve in the future.

Rahul Sharma

Abstract

Cascaded H-bridge (CHB) multilevel converter is becoming one of the most promising candidates for medium voltage and high power application owing to its features like modularity, scalability, low dv/dt , good power quality and fault tolerant ability. It is a very suitable converter to be used in medium voltage applications like the integration with large scale PV system and medium voltage motor drives. In this thesis, various challenges during the operation of CHB converter for such applications are discussed.

One of the requirements of a large-scale photovoltaic (PV) system connected to MV grid is to have both active and reactive power exchange capability along with balanced currents supply to the grid. However, this poses a challenge for the CHB converter because of the unbalanced power generation among the clusters or cells due to variation in radiation level, temperature, dusting on PV cells etc. In order to inject balanced power (and current) to the grid, a controlled exchange of reactive power is proposed so that the converter can work with unbalanced power generation within the clusters. The magnitude of reactive power exchange is derived and the necessary conditions to prevent overmodulation are discussed. In addition, the magnitude of zero sequence voltage is derived taking into account both active and reactive power exchange with the MV grid. Use of Barycentric coordinate system is introduced which helps to identify regions in the power plane where the exchange of reactive power is required.

Fault-tolerant operation is a key feature of CHB converter where the converter operates continuously with faulty bypassed cells. After bypassing the faulty cells, the number of healthy cells decreases, the available dc-link voltage reduces and active powers among the phases become unequal. As a result, the converter produces unbalanced and distorted grid currents. A novel zero-sequence voltage injection technique is proposed for balancing the grid currents and preventing overmodulation in each cell of the converter. The proposed technique extends the

reactive power capability of the converter during the post fault condition. Additionally, it also helps in achieving equal active and reactive power flow in each phase of the converter. A new PWM clamping strategy is also proposed to implement the zero-sequence voltage addition in the converter.

Another requirement for a large scale grid connected PV converter is its ability to stay connected to the grid during grid voltage sags and supplying reactive power to support the grid voltages. The CHB converter is analyzed considering balanced and unbalanced power generation among the phases as well as Low Voltage Ride Through (LVRT) operation. The aim here is to inject balanced current in the grid during unbalanced power generation and unbalanced voltage sags in the grid. An expression of zero-sequence voltage is derived to control the active power flow among the phases for maintaining dc link voltage under unbalanced power generation, during unsymmetrical voltage sags. The positive sequence current is supplied to the grid to meet the LVRT requirements while the negative sequence current is controlled to be zero. It is also ensured that the grid currents magnitude would not exceed the overcurrent rating of the converter.

Finally, a new strategy for the operation of a cascaded H-bridge converter based motor drives is proposed under the post-fault condition when the faulty cells are bypassed. During the post-fault condition, the phase voltages of the converter become unbalanced which causes unequal power handling by each healthy power cell causing an uneven rise of temperature in the cells. In the proposed strategy, the zero sequence voltage not only ensures maximum line voltage availability from the converter but additionally the power handled by each cell remains equal. A closed-loop control along with a clamped pulsewidth modulation strategy is used to maximize the line voltage and ensuring equal power handing by each cell during the postfault condition. In all the work presented in the thesis, simulation and experimental results are included to validate the proposed strategies.

सारांश

कैस्केड एच-ब्रिज (सीएचबी) मल्टीलेवल कनवर्टर मध्यम वोल्टेज और उच्च शक्ति के लिए सबसे श्रेष्ठ विकल्पों में से एक बन रहा है, जो अपनी विशेषताओं जैसे कि मॉड्युलैरिटी, स्केलेबिलिटी, कम डीवी / डीटी, अच्छी बिजली की गुणवत्ता और फॉल्ट सहिष्णु क्षमता के कारण है। यह मध्यम वोल्टेज अनुप्रयोगों में बड़े पैमाने पर पीवी सिस्टम और मध्यम वोल्टेज मोटर ड्राइव के साथ एकीकरण के रूप में उपयोग करने के लिए एक बहुत ही उपयुक्त कनवर्टर है। इस थीसिस में, ऐसे अनुप्रयोगों के लिए सीएचबी कनवर्टर के संचालन के दौरान विभिन्न चुनौतियों पर चर्चा की गयी है।

एमवी ग्रिड से जुड़े एक बड़े पैमाने पर फोटोवोल्टिक (पीवी) प्रणाली की आवश्यकताओं में से एक ग्रिड के लिए संतुलित धाराओं की आपूर्ति के साथ-साथ एक्टिव और रिएक्टिव दोनों पावर विनिमय क्षमता है। हालाँकि, यह सीएचबी कनवर्टर के लिए एक चुनौती बन जाता है क्योंकि क्लस्टर या सेल के बीच असंतुलित बिजली उत्पादन के कारण विकिरण स्तर, तापमान, पीवी सेल पर धूल आदि में भिन्नता के कारण ग्रिड को संतुलित शक्ति (और वर्तमान) इंजेक्ट करने के लिए, आदि। प्रतिक्रियाशील शक्ति का एक नियंत्रित विनिमय प्रस्तावित है ताकि कनवर्टर समूहों के भीतर असंतुलित बिजली उत्पादन के साथ काम कर सके। रिएक्टिव पावर विनिमय की परिमाण व्युत्पन्न की जाती है और अधि मॉड्यूलेशन को रोकने के लिए आवश्यक शर्तों पर चर्चा की गयी है। इसके अलावा, शून्य अनुक्रम वोल्टेज की भयावहता को एमवी ग्रिड के साथ एक्टिव और रिएक्टिव पावर विनिमय दोनों को ध्यान में रखा जाता है। केंद्रीय निर्देशांक प्रणाली का उपयोग शुरू किया गया है जो पावर प्लेन में उन क्षेत्रों की पहचान करने में मदद करता है जहां रिएक्टिव पावर का आदान-प्रदान आवश्यक है।

फॉल्ट -सहिष्णु संचालन सीएचबी कनवर्टर की एक प्रमुख विशेषता है जहां कनवर्टर लगातार गलत बाईपास सेल के साथ काम करता है। दोषपूर्ण सेल को दरकिनार करने के बाद, स्वस्थ सेल की संख्या कम हो जाती है, उपलब्ध डीसी-लिंक वोल्टेज कम हो जाता है और चरणों के बीच एक्टिव पावर असमान हो जाती हैं। नतीजतन, कनवर्टर असंतुलित और विकृत ग्रिड धाराओं का उत्पादन करता है। ग्रिड धाराओं को संतुलित करने और कनवर्टर के प्रत्येक सेल में अधि मॉड्यूलेशन को रोकने के लिए एक उपन्यास शून्य-अनुक्रम वोल्टेज इंजेक्शन तकनीक प्रस्तावित है। प्रस्तावित तकनीक पोस्ट गलती की स्थिति के दौरान कनवर्टर की रिएक्टिव पावर क्षमता का विस्तार करती है। इसके अतिरिक्त, यह कनवर्टर के प्रत्येक चरण में समान एक्टिव और रिएक्टिव पावर प्रवाह प्राप्त करने में भी मदद करता है। एक नई पीडब्लूएम क्लैम्पिंग रणनीति भी कनवर्टर में शून्य-अनुक्रम वोल्टेज जोड़ को लागू करने के लिए प्रस्ताव है।

बड़े पैमाने पर ग्रिड कनेक्टेड पीवी कनवर्टर के लिए एक और आवश्यकता ग्रिड वोल्टेज सैंग के दौरान ग्रिड से जुड़े रहने और ग्रिड वोल्टेज का समर्थन करने के लिए रिएक्टिव पावर की आपूर्ति करने की अपनी क्षमता है। सीएचबी कनवर्टर का विश्लेषण चरणों के बीच संतुलित और असंतुलित विद्युत उत्पादन के साथ-साथ लो वोल्टेज राइड थ्रू (एल वी आर टी) ऑपरेशन पर किया जाता है। यहाँ का उद्देश्य ग्रिड में असंतुलित विद्युत उत्पादन और असंतुलित वोल्टेज सैंग के दौरान ग्रिड में संतुलित वर्तमान को इंजेक्ट करना है। शून्य-अनुक्रम वोल्टेज की अभिव्यक्ति असंतुलित विद्युत उत्पादन के दौरान असंतुलित विद्युत उत्पादन के तहत डीसी

लिक वोल्टेज को बनाए रखने के लिए चरणों के बीच एक्टिव पावर प्रवाह को नियंत्रित करने के लिए होती है। सकारात्मक अनुक्रम वर्तमान को एल वी आर टी आवश्यकताओं को पूरा करने के लिए ग्रिड को आपूर्ति की जाती है जबकि नकारात्मक अनुक्रम वर्तमान को शून्य होने के लिए नियंत्रित किया जाता है। यह भी सुनिश्चित किया जाता है कि ग्रिड धाराओं का परिमाण कनवर्टर की धारा रेटिंग से अधिक न हो।

अंत में, कैस्केड एच-ब्रिज कनवर्टर आधारित मोटर ड्राइव के संचालन के लिए एक नई रणनीति फॉल्ट के पश्चात की स्थिति के तहत प्रस्तावित की जाती है जब दोषपूर्ण सेल को बाईपास किया जाता है। गलती के बाद की स्थिति के दौरान, कनवर्टर के चरण वोल्टेज असंतुलित हो जाते हैं जो प्रत्येक स्वस्थ पावर सेल द्वारा असमान पावर को संभालने का कारण बनता है, जिससे सेल में तापमान का असमान विकास होता है। प्रस्तावित रणनीति में, शून्य अनुक्रम वोल्टेज न केवल कनवर्टर से अधिकतम लाइन वोल्टेज की उपलब्धता सुनिश्चित करता है, बल्कि इसके अलावा प्रत्येक सेल द्वारा नियंत्रित पावर बराबर रहती है। क्लैपड पल्स विड्थ मोड्यूलेशन रणनीति के साथ एक बंद लूप नियंत्रण का उपयोग लाइन वोल्टेज को अधिकतम करने के लिए किया जाता है और फॉल्ट के पश्चात की स्थिति के दौरान प्रत्येक सेल द्वारा समान पावर सौंपना सुनिश्चित करता है। थीसिस में प्रस्तुत सभी कार्यों में प्रस्तावित रणनीतियों को मान्य करने के लिए सिमुलेशन और प्रयोगात्मक परिणाम शामिल हैं।

Contents

Acknowledgements	iii
Abstract	v
सारांश	vii
1 Introduction	1
1.1 Background and Motivation	1
1.1.1 Types of High Power Converters	1
1.1.2 CHB fed Large Scale Solar PV System	5
1.1.3 CHB fed Motor Drives	9
1.2 Scope and Objectives	11
1.3 Organization of Chapters	12
1.4 Summary	13
2 Study of Solar PV System and CHB Converter for Grid Connected Solar PV and Motor Drive	15
2.1 Introduction	15
2.2 Solar PV System	15
2.2.1 Mathematic Modelling of Solar PV system	16
2.2.2 Solar PV Module Characteristics	18
2.3 Cascaded H-bridge Converter	21
2.3.1 Advantages of CHB Converter	24
2.3.2 Modulation Techniques for CHB Converter	25
2.4 Design of Grid Interfaced CHB Converter for Solar PV System	30

2.4.1	Voltage and Current Rating of the Switches	31
2.4.2	Designing of Solar PV Panels	32
2.5	Design of CHB Converter for Motor Drive	32
2.5.1	Converter VA Rating	33
2.5.2	Voltage and Current Rating of the Switch of H-bridge Converter	34
2.5.3	Voltage and Current Rating of Diode Bridge Rectifier	34
2.6	Fault Tolerant Operation of CHB Converter	35
2.7	Summery	38

3 Operation of Solar PV fed CHB Converter during Unbalanced Power Generation 39

3.1	Introduction	39
3.2	System Configuration	40
3.3	Derivation of Zero Sequence Voltage	42
3.4	Converter Voltage during Unbalanced Power Generation	46
3.5	Barycentric Coordinate System	47
3.6	Power Balancing Extension	49
3.6.1	Reactive Power Exchange	49
3.6.2	Cumulative DC link Voltage Increment	52
3.7	Control Strategy	52
3.7.1	Active and Reactive Power Control	53
3.7.2	Intercluster Balancing Control (Phase Compensation)	54
3.8	Simulation Results	54
3.9	Experimental Results	59
3.9.1	Balanced Power Generation ($P_a=P_b=P_c=300$ W, $Q_g=0$ VAR)	59
3.9.2	Unbalanced Power Generation	60
3.10	Summary	61

4 Operation of Solar PV fed CHB Converter with Bypassed Faulty Cells 63

4.1	Introduction	63
-----	------------------------	----

4.2	System Configuration	64
4.2.1	Challenges during Post-fault Condition	65
4.3	Zero Sequence Voltage Injection	66
4.4	Effect of Available DC link and Active and Reactive power Capacity of the Converter	68
4.4.1	Pre-fault Condition	70
4.4.2	Post-fault Condition	70
4.5	Novel PWM Strategy	73
4.6	Simulation Results	77
4.6.1	Pre-fault and Post-fault Condition for [10 – 9 – 8]	79
4.6.2	Post-fault Condition for [10 – 8 – 8]	80
4.7	Experimental Results	82
4.8	Summary	84
5	Fault Tolerant Operation of CHB Converter in Motor Drive Application	85
5.1	Introduction	85
5.2	Operation of CHB based Motor Drive during Faulty Cell Condition	86
5.3	Equal Power Handling among the Cells	88
5.4	PWM Strategy	93
5.5	Simulation Results	95
5.5.1	Pre-fault Condition - [5-5-5] CHB Configuration	96
5.5.2	Post-fault Condition - [5-4-3] CHB configuration	96
5.5.3	Post-fault Condition- for [5-4-4] CHB Configuration with Low Power Factor	100
5.6	Experimental Results	103
5.6.1	Pre fault condition- [3-3-3] CHB configuration	103
5.6.2	Post fault condition- [3-2-2] CHB configuration	105
5.7	Summary	108
6	Operation of Solar PV fed CHB Converter during LVRT Phenomenon	109
6.1	Introduction	109

6.2	Low voltage Ride Through Requirements	109
6.3	Power Balancing among the Phases during LVRT	112
6.4	Limitations of Solar PV fed CHB Converter during LVRT	117
6.5	Control Strategy	118
6.6	Simulation Results	120
6.7	Experimental Results	125
6.8	Summary	134
7	Conclusion and Future Scope	135
7.1	Conclusion	135
7.2	Future Scope	136
	Appendices	151
A	Experimental Prototypes	153
A.1	Laboratory Experimental Prototype for Grid Connected CHB Converter	153
A.2	Laboratory Experimental Prototype for CHB Converter for Motor Drive	154

List of Figures

1.1	High power converter classifications.	2
1.2	Multilevel converter topologies: (a) neutral point clamped converter, (b) flying capacitor converter, and (c) cascaded H-bridge converter.	3
1.3	Solar PV systems integrated to the medium voltage grid.	5
1.4	Block diagram of medium voltage motor drive.	9
2.1	(a) Cell, (b) module, (c) string, and (d) array.	16
2.2	Equivalent circuit of a practical solar PV cell.	16
2.3	Equivalent circuit of a practical solar PV module.	17
2.4	Ideal characteristic: (a) current converted by irradiation, (b) diode current, and (c) output current with reference to output voltage.	18
2.5	I-V characteristic of PV module with three remarkable labels.	19
2.6	P-V characteristics of solar PV module.	19
2.7	Solar PV characteristics with different radiation levels: (a) I-V curve (b) P-V curve.	20
2.8	Solar PV characteristics with varying temperature levels: (a) I-V curve (b) P-V curve.	21
2.9	(a) Basic block of H-bridge converter. (b) Cascaded H-bridge converter.	22
2.10	Switching states and the corresponding output voltage level of H-bridge cell.	22
2.11	Synthesis of output voltage waveform corresponding to CHB converter.	23
2.12	Circuit diagram of three phase $(2L + 1)$ level CHB converter.	24
2.13	Implementation of phase shift pulse width modulation technique for five level CHB converter.	26

2.14	Phase shift PWM: (a) modulating waveform (V_m) (b) carrier waveforms V_{c1} and V_{c2} of cell 1 and cell 2 respectively. (c) carrier waveforms for two legs in cell 1.	26
2.15	(a) cell-1 (b) cell-2 and (c) converter output voltage waveforms with their harmonic spectrum using PSPWM technique.	27
2.16	Phase disposition (PD) LSPWM technique.	27
2.17	Phase opposition disposition (POD) LSPWM technique.	28
2.18	Phase opposition disposition (POD) LSPWM technique.	28
2.19	Implementation of phase disposition LSPWM for five level CHB converter.	29
2.20	a) cell-1 (b) cell-2 and (c) converter output voltage waveforms with their harmonic spectrum using PD-LSPWM technique.	29
2.21	Grid interfaced CHB converter for solar PV application.	30
2.22	Circuit diagram of CHB fed motor drive.	33
2.23	A schematic of H-bridge with bypassed switch arrangement.	36
2.24	Circuit diagram of CHB converter: (a) [5 – 5 – 5] configuration under normal condition (b) [5 – 4 – 3] configuration with bypassed faulty cells.	37
2.25	Phasor diagram: (a) During normal condition, (b) during fault condition, (c) post fault condition with bypassing the healthy cells, (d) post fault condition with neutral shift point shift, and (e) post fault condition with maximum line voltage.	38
3.1	Three phase grid tied solar PV fed CHB converter configuration.	40
3.2	Phasor diagram of grid tied CHB multilevel converter:(a) balanced power generation (b) unbalanced power generation.	41
3.3	Schematic representation of grid interfaced CHB multilevel converter during balanced power generation.	41
3.4	Phasor diagram of grid tied solar PV fed CHB converter during unequal power generation within the clusters with zero sequence voltage injection.	43
3.5	Schematic representation of grid interfaced CHB multilevel converter with zero sequence voltage injection.	43

3.6	(a) Variation of V_z (in per unit (pu)) with power factor under different powers among the clustersn, and (b) variation of α (in radian) with power factor under different powers among the clusters.	46
3.7	Variation of peak voltage of clusters with reactive power at $P_a=1$ pu, $P_b=0.7$ pu, and $P_c=0.6$ pu.	48
3.8	Power unbalanced represented as the barycentric coordinate system: barycentre ' c_1 ' at $P_a = P_b = P_c$ and barycentre ' c_2 ' at $P_a=1$ pu, $P_b=0.3$ pu, and $P_c=0.2$ pu.	48
3.9	Waveforms of cluster voltages, DC link voltage, and zero sequence voltage for (a) $Q_g = 0$ pu, (b) $Q_g = -3.66$ pu, and (c) $Q_g = 3.66$ pu, and showed zoomed in view on the right side.	51
3.10	Power balancing region with or without reactive power exchange.	51
3.11	Power balancing regions with variation of DC link voltage (k) displayed: (a) 2-D view and (b) 3-D view.	52
3.12	Control diagram of grid tied cascaded H-bridge converter during unbalanced power generation among the cluster.	53
3.13	Simulation results without injecting zero sequence voltage: (a) active power from each cluster, (b) three-phase active power and reactive power supply to grid, (c) grid voltages, (d) grid currents, (e) phase cluster voltages, (f) zero sequence voltage (rms).	55
3.14	Simulation results:(a) active power from each cluster. (b) three-phase active power and reactive power, (c) active power delivered by zero sequence voltage, (d) reactive power delivered by zero sequence voltage, (e) grid voltages. (f) grid currents, (g) Phase cluster voltages, and (h) zero sequence voltage (rms).	56
3.15	Simulation results with varying power among the phases: (a) active power from each cluster, (b) three-phase active power (P_g) and reactive power (Q_g) supply to grid, (c) active power delivered by zero sequence voltage, (d) reactive power delivered by zero sequence voltage, (e) grid voltages, (f) grid currents. (g) phase cluster voltages, and (h) zero sequence voltage (rms).	57

3.16 Simulation results during one phase power is zero: (a) active power from each cluster, (b) three-phase active power (P_g) and reactive power (Q_g) supply to grid, (c) active power delivered by zero sequence voltage, (d) reactive power delivered by zero sequence voltage, (e) grid voltages, (f) grid currents. (g) phase cluster voltages, and (h) zero sequence voltage (rms). 58

3.17 Experimental results under balanced power generation with reactive power $Q_g=0$:(a) phase cluster voltages (100 V/div) and zero sequence voltage v_z (50 V/div), (b) grid currents (5 A/div) and grid phase voltage v_{cn} (60 V/div), and (c) active and reactive power supplied to the grid. 60

3.18 Experimental results under unbalanced power generation ($P_a=300$ W, $P_b=270$ W pu, and $P_c=240$ W): (a) phase cluster voltages (100 V/div) and zero sequence voltage v_z (50 V/div), (b) grid currents (5A/div) and grid phase voltage v_{cn} (60 V/div), and (c) active and reactive power supplied to the grid. 60

3.19 Experimental results under unbalanced power generation ($P_a=300$ W, $P_b=210$ W, and $P_c=180$ W): (a) phase cluster voltages (100 V/div) and zero sequence voltage v_z (50 V/div), (b) grid currents (5A/div) and grid phase voltage v_{cn} (60 V/div), and (c) active and reactive power supplied to the grid (inductor symbol: leading power factor). 61

3.20 Experimental results under unbalanced power generation ($P_a=300$ W, $P_b=180$ W, and $P_c=210$ W): (a) phase cluster voltages (100 V/div) and zero sequence voltage v_z (50 V/div), (b) grid currents (5A/div) and grid phase voltage v_{cn} (60 V/div), and (c) active and reactive power supplied to the grid (capacitor symbol: leading power factor). 61

4.1 Configuration of solar PV fed CHB converter interfaced with Three-phase grid. . 64

4.2 Schematic diagram of grid interfaced CHB converter for solar PV application during the post fault condition. 66

4.3 Phasor diagram with faulty cell in phase a cluster. 66

4.4	Variation of peak value of cluster voltages with reactive power exchange with the grid : (a) pre-fault, (b) post fault condition $[A - B - C] = [10 - 9 - 8]$, and (c) extended linear modulation region with fault condition $[A - B - C] = [10 - 9 - 8]$	72
4.5	PQ diagram of the converter.	73
4.6	Block diagram of PWM clamping strategy.	74
4.7	Waveforms for $[A - B - C] = [10 - 9 - 8]$: (a) Reference voltages for converter (v_{xo}), and (b) waveforms of modified reference (v_{xo}^*) and modified zero sequence voltage ($v_{z,1}$) using clamping strategy.	75
4.8	Movement of converter neutral point before and after clamping.	75
4.9	Control diagram of grid connected CHB converter during fault with exact zero sequence voltage tracking.	76
4.10	Waveforms for $n_a = 0, n_b = 1, n_c = 2$ modified references (v_{xo}^*) and modified zero sequence voltage ($v_{z,1}$) using proposed control method	76
4.11	Simulation results for $[A - B - C] = [10 - 9 - 8]$: (a) active power of each cluster, (b) grid voltages, (c) grid currents, (d) three phase active and reactive power, (e) cluster voltages, (f) reference voltage for the clusters, (g) zero sequence voltage, and (h) DC link voltage of each cluster.	78
4.12	Simulation results for $[A - B - C] = [10 - 8 - 8]$: (a) active power of each cluster, (b) grid voltages, (c) grid currents, (d) three phase active and reactive power, (e) cluster voltages, (f) reference voltage for the clusters, and (g) DC link voltage of each cluster.	80
4.13	Simulation results for $[A - B - C] = [10 - 8 - 8]$ with lagging power factor: (a) active power of each cluster, (b) grid voltages, (c) grid currents, (d) three phase active and reactive power, (e) cluster voltages, (f) reference voltage for the clusters, and (g) DC link voltage of each cluster.	81

4.14	Waveforms for $[A - B - C] = [3 - 3 - 3]$ at unity power factor: (a) cluster voltages (100 V/div) and zero sequence voltage (100 V/div), (b)three phase grid currents (10 A/div) and grid voltage (100 V/div)), and (c) active and reactive power supplied the grid.	83
4.15	Waveforms for $[A - B - C] = [3 - 3 - 2]$ with injection of reactive power without PWM clamping strategy: (a) reference voltages and zero sequence voltage, (b) cluster voltages (100 V/div) and zero sequence voltage (100 V/div), (c) line voltages of the converter (200 V/div), (d)three phase grid currents (10 A/div) and grid voltage (50 V/div)), and (e) active and reactive power supplied into the grid.	83
4.16	Waveforms for $[A - B - C] = [3 - 3 - 2]$ with injection of reactive power without PWM clamping strategy: (a) reference voltages and zero sequence voltage, (b) cluster voltages (100 V/div) and zero sequence voltage (100 V/div), (c) line voltages of the converter (200 V/div),(d)three phase grid currents (10 A/div) and grid voltage (50 V/div)), and (e) Active and reactive power supplied into the grid.	84
5.1	$2L + 1$ level CHB multilevel converter with motor load.	87
5.2	Phasor diagram under: (a) Pre-fault condition. (b) fault condition. (c) Post fault condition.	87
5.3	Phasor diagram under faulty cell in phase a of the converter.	89
5.4	Schematic representation of converter based motor drive under faulty cell condition.	90
5.5	(a) Position of the converter neutral point in the maximum line voltage triangle for different power generation ($P_a - P_b - P_c$) in the case of [5-4-4] CHB configuration. (b) Zoomed view.	92

5.6 Waveforms for [5-4-4] CHB configuration: (a) load phase voltage (v_{xn}) (dotted line), zero sequence voltage (v_z) and reference voltage for converter (v_{xo}), (b) modified reference (v_{xo}^*) and reference voltage (v_{xo}), and (c) modified zero sequence voltage. 94

5.7 Movement of the converter neutral point before and after the clamping method in case of [5-4-4] CHB configuration. 95

5.8 Proposed strategy for obtaining correct value of zero sequence voltage for equal power handling in each cell. 95

5.9 (a)Reference voltage before clamping method in dotted line and modified reference voltage in firm lines and (b) zero sequence voltage. 95

5.10 Simulation results for pre fault condition-[5-5-5] CHB configuration: (a) converter reference voltages, (b) zero sequence voltage, (c) cluster voltages, (d) line voltages, (e) load currents, and (f) power in each phase. 97

5.11 Line voltage triangle in case of [5-4-3] condition. 98

5.12 Simulation results for unequal power handling in post fault- [5-4-3] CHB configuration: (a) converter reference voltages, (b) zero sequence voltage, (c) cluster voltages, (d) line voltages, (e) load currents, and (f) power in each phase. 98

5.13 Simulation results for equal power handling for post fault- [5-4-3] CHB configuration: (a) converter reference voltages. (b) zero sequence voltage. (c) cluster voltages. (d) line voltages. (e) load currents. (f) power in each phase. 99

5.14 Frequency spectrums during equal power handling: (a) v_{an} , (c) v_{bn} , and (d) v_{cn} . 99

5.15 Frequency spectrums during equal power handling: (a) v_z^* , (b) v_{an}^* , (c) v_{bn}^* , and (d) v_{cn}^* 100

5.16 Line voltage triangle for [5-4-4] condition. 100

5.17 Simulation results for post fault-[5-4-4] CHB configuration when one phase power is zero at low power factor: (a) converter reference voltages, (b) zero sequence voltage, (c) cluster voltages. (d) line voltages, (e) load currents, and (f) power in each phase. 101

5.18 Simulation results for equal power handling in Post fault-[5-4-4] CHB configuration at low power factor: (a) Reference voltages, (b) zero sequence voltage, (c) cluster voltages, (d) line voltages, (e) load currents, and (f) power in each phase. 102

5.19 Experimental Waveforms during balanced condition: (a) reference voltages (2V/div) and (b) zero sequence voltage (2V/div). 103

5.20 Experimental Waveforms for pre fault-[3-3-3] CHB configuration: (a) cluster voltages (100 V/div)and (b) phasor of cluster voltages. 104

5.21 Experimental Waveforms during for pre fault-[3-3-3] CHB configuration: (a) line Voltages (200 V/div) and (b) load currents (5 A/div). 104

5.22 Total power of the load 104

5.23 Experimental Waveforms during unequal power generation in post fault [3-2-2] CHB configuration: (a) reference voltages (2V/div) and (b) zero sequence voltage (2V/div). 105

5.24 Experimental Waveforms during unequal power generation in post fault [3-2-2] CHB configuration:(a) Cluster Voltages (100 V/div). (b) phasor of cluster voltages. 105

5.25 Experimental Waveforms during unequal power generation in post fault [3-2-2] CHB configuration: (a)line Voltages (200 V/div) and (b) load currents (5 A/div).105

5.26 Power for: (a) phase cluster *a*, (b) phase cluster *b*,(c) phase cluster *c*, and (d) Load. 106

5.27 Experimental Waveforms during equal power generation in post fault [3-2-2] CHB configuration: (a) reference voltages (2V/div) and (b) zero sequence voltage (2V/div). 106

5.28 Experimental Waveforms during equal power generation in post fault [3-2-2] CHB configuration:(a) cluster Voltages (100 V/div) and (b) phasor of cluster voltages. 107

5.29 Experimental Waveforms during equal power generation in post fault [3-2-2] CHB configuration:(a) line Voltages (200 V/div) and (b) load currents (5 A/div).107

5.30	Power for: (a) phase cluster a , (b) phase cluster b , (c) phase cluster c , and (d) Load.	107
6.1	LVRT characteristics according to German grid code: (a) grid voltage with respect to fault duration (s) and (b) reactive component of the grid current requirement in correspond with voltage sag.	110
6.2	Circuit configuration of grid interfaced solar PV fed CHB converter.	112
6.3	Phasor diagram of solar PV fed CHB converter integrated with grid under unsymmetrical voltage sag and unequal PV power generation among the phases.	113
6.4	Limitation for the balance grid currents under LVRT in power plane.	118
6.5	Overall controller for CHB converter for solar PV application.	119
6.6	Implementation of fortescue operator in Time domain.	119
6.7	Simulation results during symmetrical voltage sag with balanced power generation: (a) active power and reactive power supplied to grid, (b) grid voltages, (c) grid currents, and (d) converter voltages.	122
6.8	Simulation results during Symmetrical voltage sag with unbalanced power generation ($P_a = 1$, $P_b = 0.9$ and $P_c = 0.8$ pu: (a) Per phase powers, (b) total grid active and reactive power, (c) grid voltages, (d) Grid currents, and (e) converter voltages, (d) DC link voltages, and (g) zero-sequence voltage.	123
6.9	Operation of solar PV fed CHB converter under symmetrical voltage sags for balanced power generation: (a) active powers from the clusters, (b) total active and reactive power, (c) grid voltages. (d) grid currents, (e) converter voltages, (f) DC link voltages, and (g) zero sequence voltage.	124
6.10	Operation of solar PV fed CHB converter under unsymmetrical voltage sags for unbalanced power generation: (a) active powers from the clusters, (b) total active and reactive power, (c) grid voltages. (d) grid currents, (e) converter voltages, (f) DC link voltages, and (g) zero-sequence voltage.	125

6.11	Operation of solar PV fed CHB converter under unsymmetrical voltage sag for zero active power generation: (a) active powers from the clusters, (b) total active and reactive power, (c) grid voltages. (d) grid currents, (e) converter voltages, (d) DC link voltages, and (g) zero sequence voltage.	126
6.12	Waveforms of grid voltage (60 V/div.) and grid current (10 A/div.) during grid transient (x-axis: 400 ms/div): (a) unity power factor, (b) lagging power factor, and (c) unity power factor.	127
6.13	Waveforms of grid voltage (60 V/div.) and grid currents (10 A/div.) during grid transient (x-axis: 200 ms/div) during unbalanced cluster power: (a) unity power factor, (b) lagging power factor, and (c) unity power factor.	127
6.14	Waveforms of converter voltage and zero sequence voltage (100 V/div.) : (i) at unity pf,(ii) at lagging, and (iii) again at unity pf (x-axis: 200 ms/div).	128
6.15	Waveforms of grid voltages (50 V/div.) and grid current i_c (5 A/div.) before and after the voltage sag when $P_a = P_b = P_c$ (x-axis: 110 ms/div.).	128
6.16	Waveforms of grid voltage v_{cn} (50 V/div.) and grid currents (5 A/div.) during normal and LVRT condition (x axis: 94 ms/div).	129
6.17	Waveforms of input powers (100 V/div.): (a) Normal condition ($P_a \simeq P_b \simeq P_c \simeq 300$ W) and (b) LVRT condition ($P_a \simeq P_b \simeq P_c \simeq 288$ W) (x-axis: 20 ms/div).	129
6.18	Waveforms of converter voltage (100 V/div) and zero sequence voltage reference (50 V/div.): (a) Normal condition and (b) LVRT condition (x-axis: 5 ms/div).	130
6.19	Waveforms of active and reactive power (500 V/div.): (a) Normal condition ($P_g \simeq 900$ W, $Q_g \simeq 0$ VAR) and (b) LVRT condition ($P_g \simeq 860$ W, $Q_g \simeq 300$ VAR) (x-axis: 50 ms/div).	130
6.20	Waveforms of grid voltages (50 V/div.) and grid current i_c (5 A/div. before and after the voltage sag when $P_a = P_b = P_c$ (x-axis:130 ms/div.).	130
6.21	Waveforms of grid voltage v_{cn} (50 V/div.) and grid currents (5 A/div.) during normal and LVRT condition (x axis: 130 ms/div).	131

6.22	Waveforms of input powers (100 V/div.): (a) Normal condition ($P_a \simeq 300$ W, $P_b \simeq 240$ W, and $P_c \simeq 210$ W) and (b) LVRT condition ($P_a \simeq 290$ W, $P_b \simeq 232$ W, and $P_c \simeq 203$ W) (x-axis: 20 ms/div).	131
6.23	Waveforms of converter voltage (100 V/div) and zero sequence voltage reference (50 V/div.): (a) Normal condition and (b) LVRT condition (x-axis: 5 ms/div).	132
6.24	Waveforms of active and reactive power (500 V/div.): (a) Normal condition ($P_g \simeq 750$ W, $Q_g \simeq 0$ VAR) and (b) LVRT condition ($P_g \simeq 725$ W, $Q_g \simeq 430$ VAR) (x-axis: 100 ms/div).	132
6.25	Waveforms of grid voltages (50 V/div.) and grid current i_c (5 A/div.) before and after the voltage sag (x-axis: 130 ms/div)	132
6.26	Waveforms of grid voltage v_{cn} (50 V/div.) and grid currents (5 A/div.) during normal and LVRT condition (x axis: 140 ms/div).	133
6.27	Waveforms of input powers (100 V/div.): (a) Normal condition ($P_a \simeq P_b \simeq P_c \simeq 300$ W) and (b) LVRT condition ($P_a \simeq P_b \simeq P_c \simeq 0$ W) (x-axis: 40 ms/div).	133
6.28	Waveforms of converter voltage (100 V/div) and zero sequence voltage reference (50 V/div.): (a) Normal condition and (b) LVRT condition (x-axis: 5 ms/div).	133
6.29	Waveforms of active and reactive power (500 V/div.): (a) Normal condition ($P_g \simeq 900$ W, $Q_g \simeq 0$ VAR) and (b) LVRT condition ($P_g \simeq 0$ W, $Q_g \simeq 560$ VAR) (x-axis: 100 ms/div).	134
A.1	Experimental setup for grid connected CHB converter.	153
A.2	Experimental setup of cascaded H-bridge for motor drive.	155

List of Tables

2.1	Solar PV module parameters at standard test condition (STC).	20
2.2	Switching states of five level CHB converter.	23
3.1	Selection of Q_g During $P_a=1$ pu, $P_b=1$ pu and $P_c=0.4$ pu for $k=1.8$ pu.	50
3.2	Simulation parameters.	55
3.3	Experimental parameters.	59
4.1	Fundamental cluster voltages and zero sequence voltage in Figure 4.7.	74
4.2	Simulation parameters.	77
4.3	Experimental parameters.	82
5.1	Zero sequence voltages for different power handling in each phase corresponding to Figure 5.5 for [5-4-4] CHB configuration.	93
5.2	Descriptions and parameters of simulation results.	96
5.3	Parameter descriptions and values used for experimental results.	103
6.1	Simulation Parameters.	121
6.2	Experimental Parameters.	126